



This is a repository copy of *Hybrid simultaneous laser- and ultrasonic-assisted machining of Ti-6Al-4V alloy*.

White Rose Research Online URL for this paper:

<https://eprints.whiterose.ac.uk/196608/>

Version: Published Version

Article:

Dominguez-Caballero, J. orcid.org/0000-0001-7329-9929, Ayvar-Soberanis, S. orcid.org/0000-0002-1899-9743, Kim, J. et al. (3 more authors) (2023) Hybrid simultaneous laser- and ultrasonic-assisted machining of Ti-6Al-4V alloy. *The International Journal of Advanced Manufacturing Technology*, 125 (3-4). pp. 1903-1916. ISSN 0268-3768

<https://doi.org/10.1007/s00170-022-10764-5>

Reuse

This article is distributed under the terms of the Creative Commons Attribution (CC BY) licence. This licence allows you to distribute, remix, tweak, and build upon the work, even commercially, as long as you credit the authors for the original work. More information and the full terms of the licence here:

<https://creativecommons.org/licenses/>

Takedown

If you consider content in White Rose Research Online to be in breach of UK law, please notify us by emailing eprints@whiterose.ac.uk including the URL of the record and the reason for the withdrawal request.



eprints@whiterose.ac.uk
<https://eprints.whiterose.ac.uk/>



Hybrid simultaneous laser- and ultrasonic-assisted machining of Ti-6Al-4V alloy

Javier Dominguez-Caballero¹ · Sabino Ayvar-Soberanis¹ · Jin Kim² · Anish Roy² · Lin Li³ · David Curtis¹

Received: 3 August 2022 / Accepted: 22 December 2022 / Published online: 16 January 2023
© The Author(s) 2023

Abstract

The machinability of Ti-6Al-4V alloy has been a constant challenge in the industry, although the material is widely used in the aerospace and medical industries due to its mechanical properties, particularly its strength-to-weight ratio. The current research presents a hybrid laser- and ultrasonic-assisted machining (LUAM) technique to improve the machinability of Ti-6Al-4V alloy in a turning process. This is compared with ultrasonic-assisted machining (UAM), laser-assisted machining (LAM), and convectional turning (CT). The results reveal that UAM and LAM can reduce the cutting forces and surface roughness (Ra) compared to the CT. However, these are achieved mainly at the lowest range of cutting speeds. The hybrid LUAM process demonstrates process improvement with wider range of cutting speeds and depths of cut, which is achieved due to the combined force reduction and thermal softening effect by the hybrid process.

Keywords Laser-assisted machining · Ultrasonic-assisted machining · Turning · Surface roughness · Cutting forces · Ti-6Al-4V material

1 Introduction

The improvement of machinability of aerospace alloys continues to be a key area of focus in academic research and industrial development, in which the implementation of assisted machining techniques (e.g. ultrasonic, laser, electro discharge, and electro-chemical assisted machining)

have proved to have benefits in improving machinability for difficult-to-machine aerospace alloys such as nickel-based superalloys [1–3], and metal matrix composite (MMC) materials [4–6].

Titanium alloys, which are widely used for the aerospace and medical implant components due to their high strength-to-weight ratio, are also known to be ‘difficult to machine’ due to their special thermomechanical properties [7]. The improvement in the machinability of these alloys has been investigated using multiple energy field machining processes. The application of ultrasonic-assisted machining (UAM) has demonstrated improvements in machinability for high-strength alloys through high-frequency vibrations generated in one or in a combination of cutting directions, which creates oscillating loading and unloading on the cutting tool [8]. The effect of UAM has been investigated on Ti-6246 and Ti-676–0.9La [9, 10], where significant reduction of cutting forces and surface roughness compared to conventional turning (CT) at low cutting speeds from 10–30 m/min was reported. The most widely used titanium material, Ti-6Al-4V, which constitutes around 80 to 90% of use in the aerospace components [11] has also been investigated using UAM when turning. Llanos et al. [12], Zhang and Want [13], and Maroju and Pasam [14] carried out experimental investigations of force reduction during

✉ Javier Dominguez-Caballero
j.dominguez-caballero@amrc.co.uk

Sabino Ayvar-Soberanis
s.ayvar@amrc.co.uk

Jin Kim
j.w.kim@lboro.ac.uk

Anish Roy
a.roy3@lboro.ac.uk

Lin Li
lin.li@manchester.ac.uk

David Curtis
d.curtis@amrc.co.uk

¹ The University of Sheffield Advanced Manufacturing Research Centre, Sheffield, UK

² Loughborough University, Loughborough, UK

³ The University of Manchester, Manchester, UK

UAM of Ti-6Al-4V compared to CT using various cutting parameters. They found force reductions in the use of UAM, which was more evident at the lower cutting speeds. These studies did not include surface roughness analysis. Other investigations have studied the use of UAM with a heat source to induce a level of thermal softening of the workpiece. The findings suggested further machinability improvement [15, 16].

Laser-assisted machining (LAM) has also shown improvements in machinability by elevating the workpiece temperature at a short distance from the cutting edge, and thus reducing the amount of force required to cut the softened hot material [17]. Dandekar et al. [18] and Kim and Lee [19] carried out LAM experimental work for Ti-6Al-4V, comparing machinability with aspect to CT. In these two investigations, LAM was found to reduce cutting forces and improve surface roughness. In similar experimental LAM work on Ti-6Al-4V, Hedberg et al. [20], Habrat et al. [21], and Kalantari et al. [22] found an improvement in tool wear and residual stresses under certain laser processing and mechanical machining conditions, without significant detrimental effect on microstructure. Feng et al. [23] investigated LAM by developing an analytical model to predict residual stresses, where they considered the recrystallisation of the material due to the exposure to the laser beam. The model was validated with experimental milling trials on Ti-6Al-4V and Si_3N_4 materials, achieving prediction errors below 30% whilst finding a reduction of compressive residual stresses using LAM. In a similar work, Feng et al. [24] investigated the effect of LAM on surface roughness whilst milling Inconel 718 by developing a predictive analytical model based on tool movement, elastic deformation, and tool tip profile. The findings showed improvements in surface finish using LAM at certain feed rates, as well as errors below 27% and as little as 3%.

Despite various studies on multiple energy field machining of Ti alloys, very little is reported on the combination of laser- and ultrasonic-assisted machining (LUAM), and no research has been published on the implementation of these combined assisted machining processes for the turning of titanium alloys. Lin and Yang [25] investigated the effect of LUAM for Inconel 718 during milling. They found that the surface roughness was reduced with LAM and LUAM processes, as well as cutting force reduction. However, as feed rate increases, these benefits reduce. The implementation of UAM was through biaxial ultrasonic vibration of the workpiece rather than the cutting tool with an elliptical toolpath. Jiao et al. [26] implemented LUAM for the turning of tungsten carbide (YG20) and compared this with CT, LAM, and UAM. They found that LUAM had improved surface quality and reduced cutting forces. They identified the

effect of turning feed rate and laser power on surface roughness, finding that lowering feed was central to lowering Ra values. However, their comparison between the assistive technologies was limited to one set of machining parameters at a cutting speed of 15 m/min, a depth of cut of 10 μm and a feed rate of 0.01 mm/rev. In another study [27], they implemented a design of experiments, where a genetic algorithm (GA) was used to optimise material removal rate (MMR) under certain Ra limits, but this was only investigated for the LUAM at cutting speeds between 10 and 25 m/min. Research by Khajazadeh et al. [28] explored the use of UAM, LAM, and LUAM applied to the turning of a 4340 steel alloy through various designs of experiments to understand the relationships between cutting and hybrid process parameters on cutting force and surface finish. They found that LAM was more effective than LUAM in improving surface finish. Simultaneous application of laser and ultrasonic elliptical vibrations showed benefits in a considerable reduction of cutting force and acceptable improvement in surface finish. However, their study was also limited to low cutting speeds between 16 and 22 m/min. It should be noted that these investigations on LUAM applied to turning did not provide a baseline of surface quality using commercial standard tools. Kim et al. [29] carried out an experimental study on turning of aluminium metal matrix composite material using CT, UAM, LAM, and LUAM. They varied laser powers in the range of 647 and 1078 W. They observed the highest cutting force reductions in the LUAM at the highest laser power. The use of LAM alone did not reduce the cutting force due to the built-up edge (BUE) on the cutting tool, which was avoided when adding the vibration from the ultrasonic system. Surface roughness was also improved under the highest laser power in LUAM. However, BUE appeared to have affected surface roughness on all LAM conditions and the lowest laser-powered LUAM. This study was limited to one cutting speed, which was kept constant at 30 m/min.

The current research reports on the application of LUAM in turning Ti-6Al-4V alloy for the first time to understand its effect on the cutting forces and surface roughness. A special ultrasonic cutting head was developed. A full factorial experimental design was used for CT, UAM, LAM, and LUAM using cutting speeds from 20 to 70 m/min at different depths of cut. The experimental tests covered a greater range of cutting speeds compared to those presented in previous research with LUAM. This study expanded the design space of the experimental trials close to commercial cutting conditions for Ti-6Al-4V alloys. Additionally, this research included a benchmarking of the custom-made ultrasonic toolholder with commercial toolholders to better investigate these technologies for industrial applications.

2 Experimental methodology

2.1 Experimental machining setup

The laser- and ultrasonic-assisted machining (LUAM) for the turning process was carried out in a Mori Seiki NT5400 CNC turn-mill machine. Details of the experimental setup are shown in Fig. 1, which consisted of (a) apparatus setup, (b) cutting configuration, (c) schematic side view of the piezoelectric transducer, and (d) orientation of the insert. It should be noted that the machine tool configuration allowed the B-axis milling/ turning spindle to be used to hold the ultrasonic transducer cutting tool, which was designed for orthogonal cutting, whilst the machine’s indexable driven turret was used to hold the laser. This setup also permitted

a synchronised movement of the cutting tool and the laser through a single CNC programme which controlled the motion of the spindle in the Z-axis and the drive turret as well as the workpiece spindle.

The workpiece was a cylindrical bar of standard Ti-6Al-4V with an initial diameter of 77 mm and 215 mm in length. For each turning test, a new Sandvik cemented carbide insert (DCMT 11 T3 02-MF 1105) was used. These cutting tools have a PVD TiAlN coating, a corner radius of 0.4 mm, and a clearance angle of 7 deg. Force and temperature were monitored using a Kistler dynamometer Type 9129 AA (mounted to a Capto C8-based adaptor and positioned between the spindle and the ultrasonic transducer assembly) and an AGEMA 550L thermal camera with an emissivity of 0.4, respectively. Details of the developed ultrasonic tool

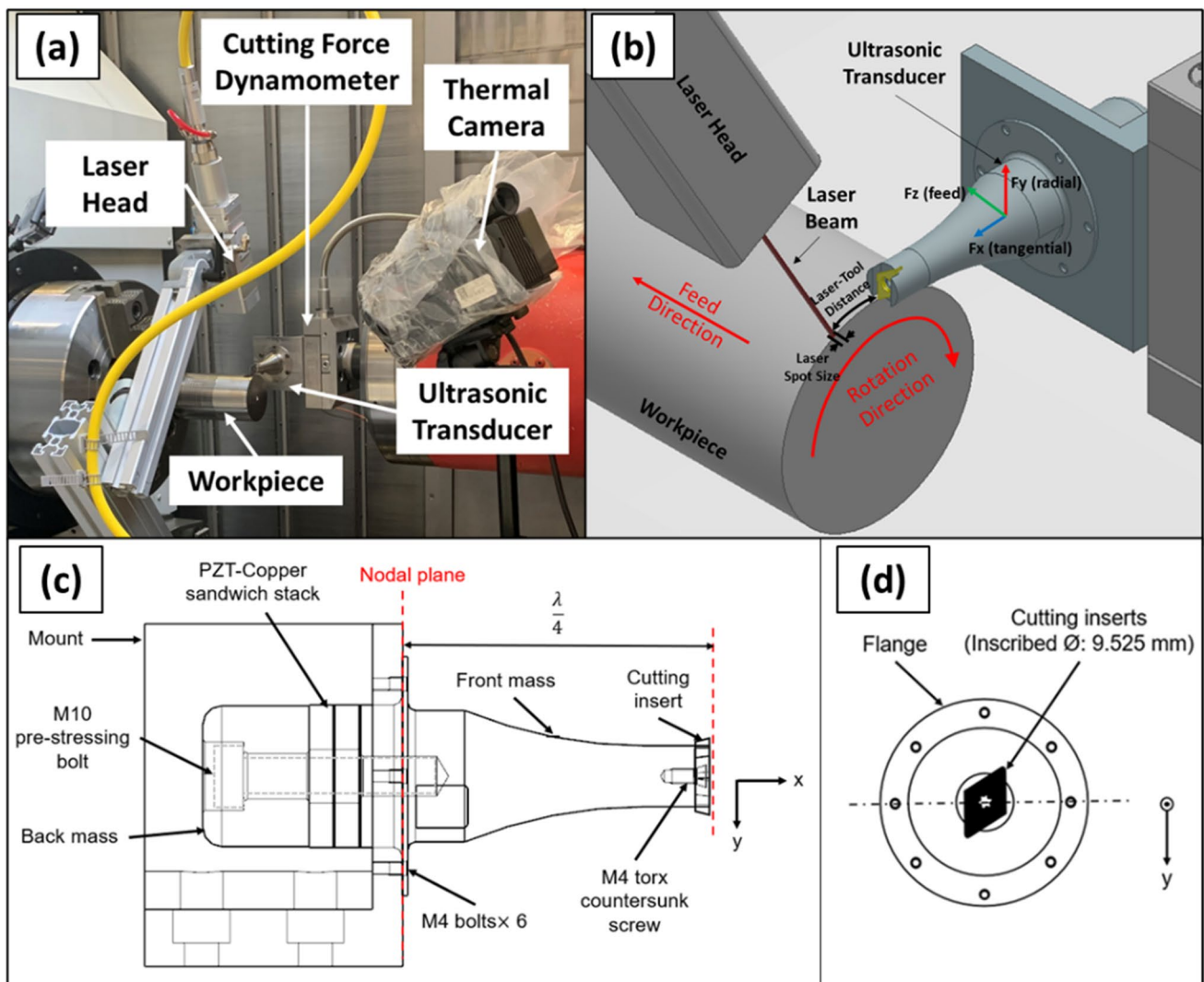


Fig. 1 Laser- and ultrasonic- assisted machining (LUAM): **a** apparatus setup, **b** cutting configuration, **c** schematic side view of the piezoelectric transducer, and **d** orientation of the insert

holder, commercial tool holders used for benchmarking and laser equipment are described in the following sections.

2.2 Laser and ultrasonic setup

The hybrid LAM technology consists of using a high-power laser to input thermal energy onto the material at a short distance from the cutting tool. The localised heating of the workpiece by the laser ensures a small heat-affected zone whilst reducing the yield strength of the volume of material prior to the cutting edge. This material softening results in a change in the chip compression ratio, thus improving the machinability of the material by reducing cutting forces [30]. In a turning operation, the LAM setup can be more controllable due to the continuous engagement between the tool and the workpiece, where the laser can follow the cutting tool in the feed direction [31].

The laser used in the experimental work was a nLight CFL-1000 continuous-wave fibre laser with a wavelength of 1070 nm, and a maximum power of 1 kW. The laser beam was focused with a FiberMINI ST processing head with a focal length of 200 mm and a ~0.7 mm spot size. The laser head was mounted onto a customised adaptable fixture to vary the spot size and the laser-tool distance (laser beam distance in advance of the rake face), as illustrated in Fig. 1a and b.

The custom-made ultrasonic cutting head consisted of an in-house manufactured Langevin-type bolt clamped piezoelectric ultrasonic transducer made of Ti-6Al-4V front and back masses and a steel mount. The ultrasonic vibration generated by PZT-copper sandwich stacks was amplified with a Sonic systems L100 auto-resonance power generator fine-tuned to an amplitude of 8 μm . Figure 1c shows a schematic side view of the piezoelectric transducer, demonstrating the assembly of the ultrasonic cutting head. The transducer was designed to resonate at 20.33 kHz. The vibration amplitude (peak-to-peak) at the tip was 28.8 μm , 7.2 μm , and 8.1 μm in tangential (F_x), radial (F_y), and feed (F_z) directions, respectively. The wavelength, λ , is obtained from:

$$\lambda = \frac{c_s}{f} \quad (1)$$

where c_s is the speed of sound in a waveguide and f is the desired resonance frequency. The exponential horn was designed such that a distance of $\frac{\lambda}{4}$ coincides with the nodal plane, allowing for maximum vibration at the transducer tip. Figure 1d shows the front view of the transducer, demonstrating the tool's location and orientation. The tool holder included a recess for the turning insert geometry type of inscribed diameter of 9.525 mm, which was aimed to achieve a secure and repeatable location of the insert. The selection of the cutting insert was crucial since the vibration was sensitive to mass. The orientation of the insert was positioned

with a rake angle of 0° when turning the outer diameter of the workpiece. However, forces in the radial direction were observed which might be related to the potential stiffness of the ultrasonic tool holder, as stated below in Section 3.2.

The transducer was mounted on a Kistler dynamometer Type 9129 AA with a charge amplifier Type 5070 to measure cutting forces at a sampling frequency of 5 kHz. The cutting force data was measured for the tangential, radial, and feed directions.

For effective ultrasonic vibration-assisted machining, tool separation during every vibratory motion is expected. From a one-dimensional tool-workpiece interaction analysis (where all lateral vibrations are ignored as these are typically small), a relation between critical cutting speed as a function of vibration characteristics can be derived. The critical cutting speed is related to machining parameters as,

$$v_c = 2\pi af; v = \pi nD \quad (2)$$

where, v_c is the critical velocity above which ultrasonically assisted machining is not expected to yield any meaningful force reduction and in effect reduces to a conventional machining process. Here, a is the amplitude of vibration, n the rotational speed of the lathe, D the workpiece diameter being machined and v the imposed speed of the machine. For effective UAT, $v_c > v$ is expected.

The power of a transducer is related to its acoustic impedance, angular frequency, and square of the amplitude. When the transducer is in active machining mode with intermittent contact with the workpiece material, the effective power is related to cutting/reaction force due to contact and the relative approach velocity. The frequency and amplitude are essentially linearly related to the power in machining. Previous numerical studies have been carried out on the effect of vibration and frequency [32] which indicate that with an increase in vibration amplitude there is an increase in equivalent plastic strain and process zone temperature which can potentially increase tool wear and BUE formation. The design of transducers is performed to ensure a range of working frequencies at which there is resonance in the primary axial mode of vibration.

2.3 Experimental methodology

Preliminary experiments were carried out to select the optimum laser spot size, laser power, and laser-tool distance. The laser processing parameters are presented in Table 1.

Firstly, to select a spot size that could generate adequate laser absorption and heating zone size, the surface of the workpiece in static condition (not rotating) was heated with the laser beam for 1.5 s. This was done using different spot sizes from 1.5 to 3 mm and various laser powers between 60 and 750 W. Maximum temperature values were calculated

Table 1 Laser characterisation parameters and values

Parameter	Values
Laser power (W)	60, 80, 100, 200, 300, 400, 600, 750
Spot size (mm)	1.5, 2, 2.5, 3
Laser-tool distance (mm)	8, 12, 17
Surface speed (m/min)	20, 45, 70

from the raw temperatures captured by the thermal camera during these tests to show the maximum thermal effect of the laser and the various spot sizes, as shown in Fig. 2a. Then the parameters were examined in a rotating condition of the workpiece to emulate the cutting conditions without any material subtraction. The tests were carried out at cutting speeds of 20, 45, and 70 m/min, where the maximum cutting speed was based on the ultrasonic tool's critical speed. However, for these tests and for the remaining trials, mean temperature values were calculated from the raw temperature data, as shown in Fig. 2b. Finally, the selection of the laser-tool distance consisted of using the spot size and laser power selected in the previous steps, as well as a cutting speed of 30 m/min, feed per revolution of 0.15 mm/rev, and a depth of cut of 0.2 mm. These selected laser parameters were then used during the LAM and LUAM turning trials.

Initial benchmarking cutting tests were also carried out using the developed ultrasonic tool holder and commercial turning tool holders from Sandvik prior to investigating the hybrid turning processes. This was carried out to assess the rigidity of CT with the custom-made

ultrasonic tool holder setup compared to commercial cutting conditions, and thus provide a benchmark for the results obtained using the same ultrasonic tool setup with the assistive technologies (UAM, LAM, and LUAM). The commercial tool holders included an oblique cutting (C6-SDJCL-45065-11C) and an orthogonal cutting test (STFCR 2020 K 11-AB1). Recommended industrial cutting parameters for the finishing processes were utilised as follows: feed per revolution of 0.04 mm/rev, depth of cut of 0.25 mm, and cutting speeds of 20, 45, and 70 m/min, where the maximum cutting speed was tested to investigate the ultrasonic tool's critical speed.

The benchmarking tests were performed with and without flood coolant to assess the impact of wet and dry cutting conditions on the surface roughness, given that the ultrasonic and laser systems were designed to work in dry conditions, the relevant results of the benchmark experiments are presented in Section 3.2. Finally, the main investigation into hybrid turning was carried out based on a full factorial design of experiments (DoE) as presented in Table 2, where the test centre point was repeated three times (test no. 5, 6, and 7) to provide a measure of process stability and inherent variability. Each turning test had a cutting length of 40 mm including all the hybrid processes, where the ultrasonic and laser systems were active for 10 mm of the cutting length, respectively. Fresh tools were used during each test at dry conditions. Cutting forces and temperature were monitored during the trials, and the surface roughness was measured after-cut using a Mitutoyo SJ-210 surface roughness tester with a stylus of 5 μm tip radius, the results of experiments are presented from Section 3.3 to Section 3.5.

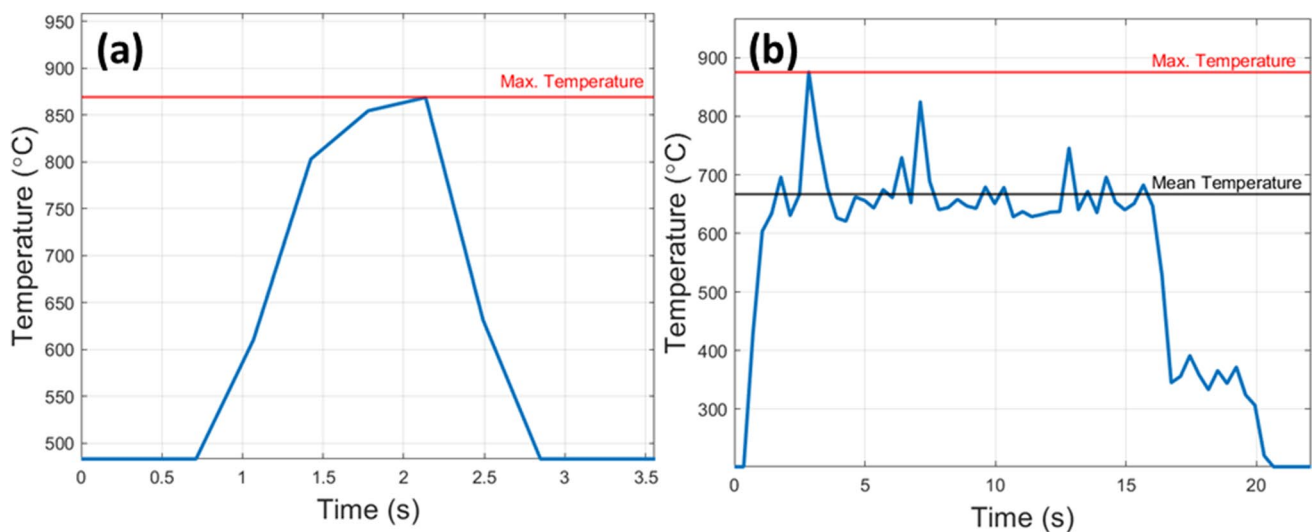
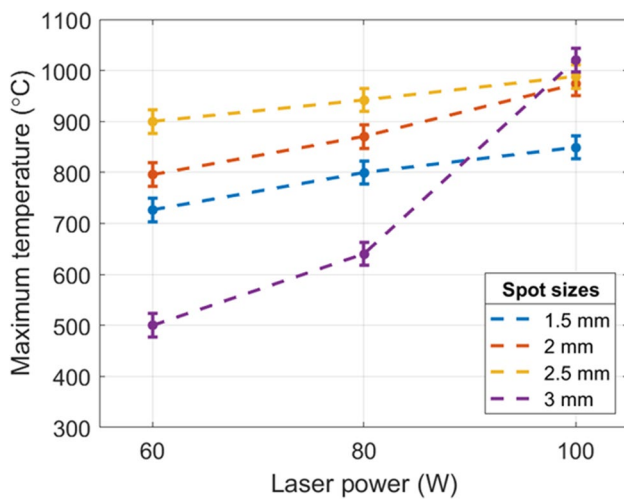
**Fig. 2** Examples of raw temperatures for **a** spot size selection and **b** laser power selection

Table 2 DoE cutting parameters for turning trials

Test no	Cutting speed, V_c (m/min)	Depth of cut, a_p (mm)	Feed per revolution, f_n (mm/rev)
1	70	0.25	0.04
2	45	0.25	0.04
3	20	0.25	0.04
4	70	0.2	0.04
5	45	0.2	0.04
6	45	0.2	0.04
7	45	0.2	0.04
8	20	0.2	0.04
9	70	0.15	0.04
10	45	0.15	0.04
11	20	0.15	0.04

**Fig. 3** Maximum temperatures during static (1.5 s) laser exposure for various spot sizes

3 Results and discussion

3.1 Effect of laser irradiation

The resulting maximum temperatures reached by the laser irradiation at different beam spot sizes are shown in Fig. 3. The diameters of 2 and 2.5 mm presented the most stable profiles and the highest temperature values, which also produced the least workpiece surface evaporation after the laser exposure of 80 W as shown in Figs. 4b and c. Note that the workpiece surface evaporation occurred at the laser spot size diameter of 1.5 mm, whilst the 3 mm spot size diameter did not achieve good absorption as illustrated in Fig. 4a and d, respectively.

The mean temperatures recorded using the narrowed-down spot sizes of 2 and 2.5 mm on the rotating workpiece surface for the different surface speeds and laser powers

are shown in Fig. 5. Although higher temperatures were expected to produce a better material softening, temperatures above 880 °C could also cause a phase transformation, which would have a detrimental impact on the surface integrity of the Ti-6Al-4V material [1]. In this study, the laser power of 750 W with a spot size of 2 mm was able to maintain the temperatures between 576 and 830 °C on the part across the different speeds, thus these parameters were selected for further testing. Other laser parameters produced either much lower temperatures than the selected range or higher than the phase transformation limit.

The results of the laser-tool distance selection in Fig. 6a demonstrated that a distance of 8 mm generated excessive chip burning, which was probably caused by the excessive heat energy dissipated by the swarf. A distance of 17 mm generated very low chip burning as illustrated in Fig. 6c, but low temperatures were registered at the cutting edge. Finally, the laser-tool distance of 12 mm was selected as it produced very low chip burning as shown in Fig. 6b, whilst maintaining a high temperature at the cutting edge of between 500 and 600 °C.

3.2 Initial benchmarking

The surface roughness (R_a) results from the benchmarking tests for all cutting parameters are presented in Fig. 7 at a feed per revolution of 0.04 mm/rev, a depth of cut of 0.25 mm, a cut length of 10 mm, and cutting speeds of 20, 45, and 70 m/min under dry and wet cutting conditions. These parameters were selected in accordance with the limits recommended by the carbide insert tooling supplier. The cutting tests using the ultrasonic tool holder were carried out with the ultrasonic system switched off during the cuts, which enabled conventional turning to be performed with this tool holder. It should be noted that the ultrasonic tool holder was used without flood coolant during the benchmarking tests to avoid any potential damage to the system. The tool holder was designed to work in dry conditions; therefore, it was not manufactured to prevent coolant penetration. The surface roughness produced by the commercial tool holders produced R_a values of between 0.66 and 0.82 μm across the cutting speeds and coolant conditions. The ultrasonic tool holder with a CT setup produced higher R_a values between 1 and 1.2 μm . These differences in surface quality showed that there was a potential stiffness issue on the ultrasonic tool holder due to its cantilever design; further research is needed to improve this.

When the cylindrical bar was machined at higher feed rates above the tool supplier recommendation, as shown in Fig. 8 at a speed of 45 m/min, it was observed that the difference in surface roughness between the commercial and customised tools was significantly reduced. This was an indication of the greater effect of the feed rate, which dominates the peak-to-peak topography of the R_a response, over the

Fig. 4 Workpiece surface for laser exposure of 80 W for spot diameters of **a** 1.5 mm, **b** 2 mm, **c** 2.5 mm, and **d** 3 mm

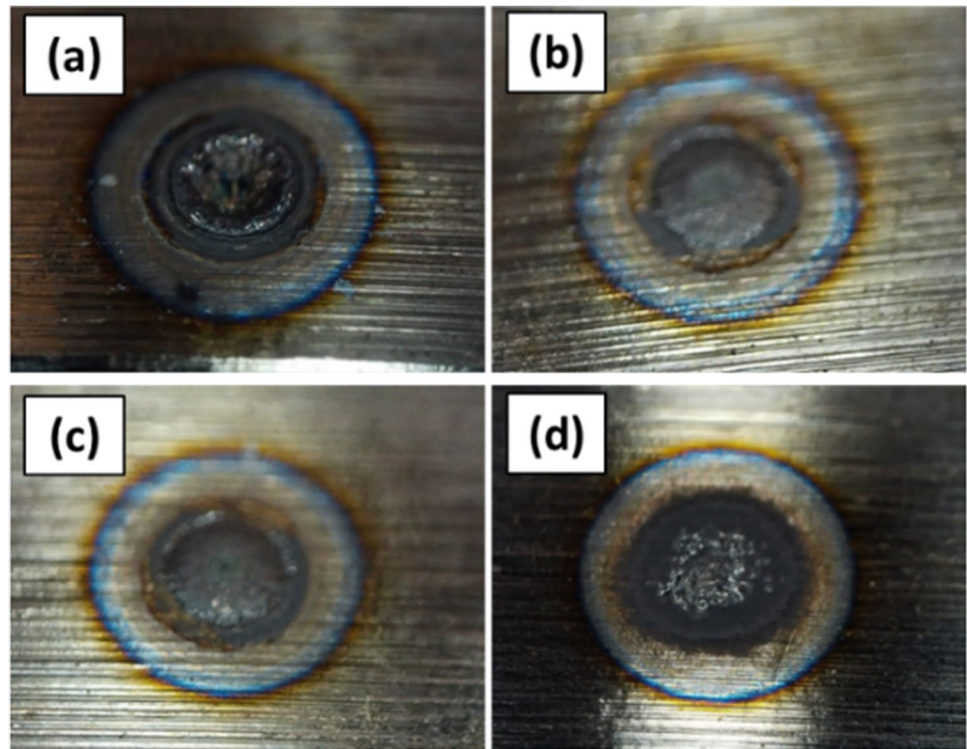
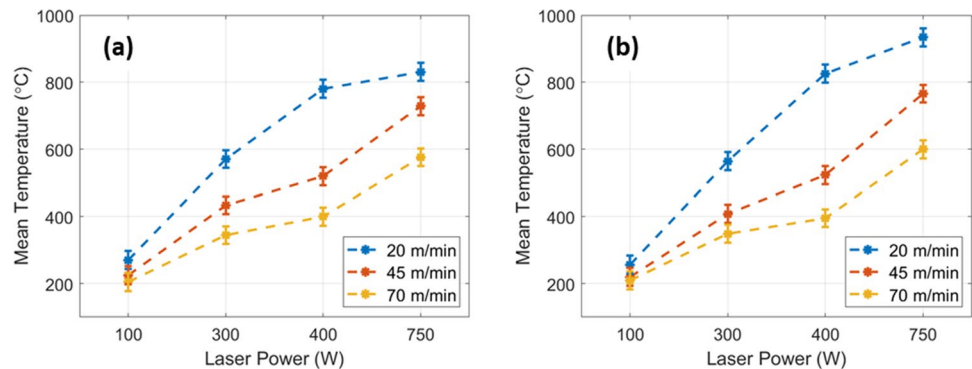


Fig. 5 Maximum temperatures for various laser powers at the different surface speeds for **a** 2 mm and **b** 2.5 mm spot sizes



stiffness issues of the customised tool. Therefore, given that the feed per revolution of 0.04 mm/rev is the recommended value by the tool supplier for the carbide cutting insert, this value was used as the baseline in this study.

3.3 Hybrid turning: cutting forces

As shown in the cutting force diagram of Fig. 9, the experiments were carried out to start with a conventional turning (CT) operation, followed by the activation of ultrasonic-assisted machining (UAM), then by activating the laser to implement the combined laser- and ultrasonic-assisted machining (LUAM), and finally, the UAM was deactivated to use only the laser-assisted machining (LAM). This procedure allowed a clear understanding of the contribution of each assistive technology.

The raw signals of the cutting forces were processed with MATLAB software to obtain the mean cutting force values. The graphs in Fig. 10 illustrate the effect of the hybrid processes and range of machining parameters on the tangential, radial, and feed direction cutting forces. The dashed lines in each graph correspond to the force values recorded for LUAM for each cutting speed for a better visualisation when it is compared to other combinations. The error bars of the cutting forces represent the standard deviation of the repeated centre points of the design of experiments. No data outliers were removed from the force results, which was significant with p values below 0 at a 95% confidence level.

In terms of the cutting parameters, in general, the forces presented similar magnitudes for the same cutting conditions. It showed that the variation of surface speed did not

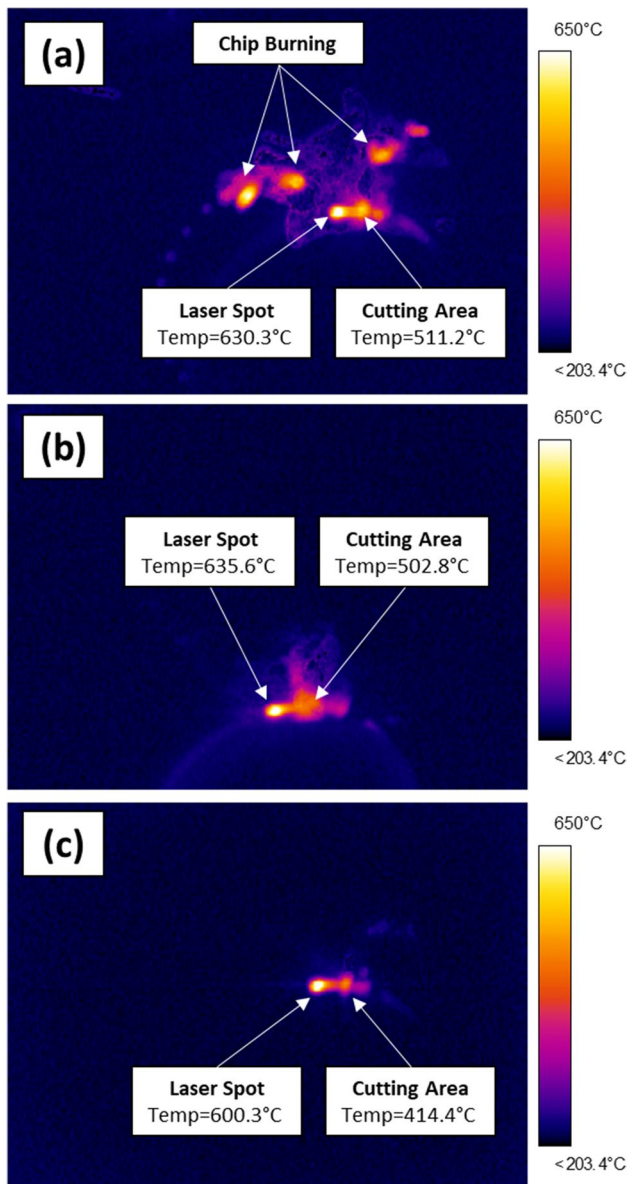


Fig. 6 Thermal images for laser-tool distance of **a** 8 mm, **b** 12 mm, and **c** 17 mm

have a significant effect on the cutting forces for the conventional machining trials. However, the effect on the cutting forces was mainly driven by the changes in depth of cut (DoC), with a trend of decreasing the magnitudes approximately 50% from the highest DoC 0.25 mm to the lowest DoC 0.15 mm when maintaining the other cutting parameters at the same conditions.

It was observed that the change in cutting speed exhibited a decrease on the cutting forces specially for the UAM and LUAM conditions, with similar tendencies of reducing the forces by up to 50% for the lowest DoC 0.15 mm and surface speed 20 m/min whilst keeping the same cutting conditions.

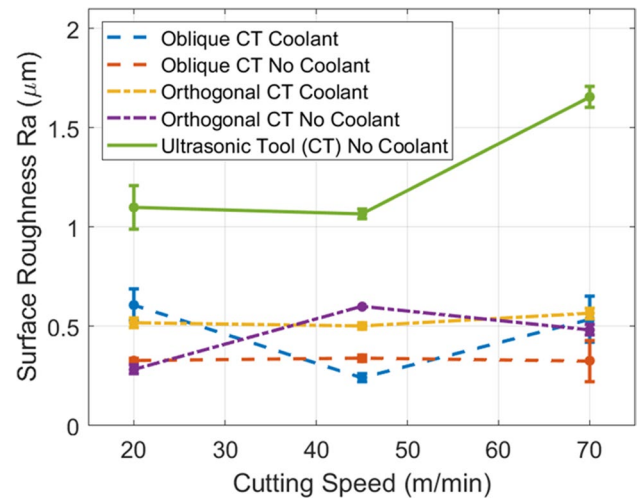


Fig. 7 Surface roughness results for benchmarking tests for feed per revolution of 0.04 mm/rev at different cutting speeds

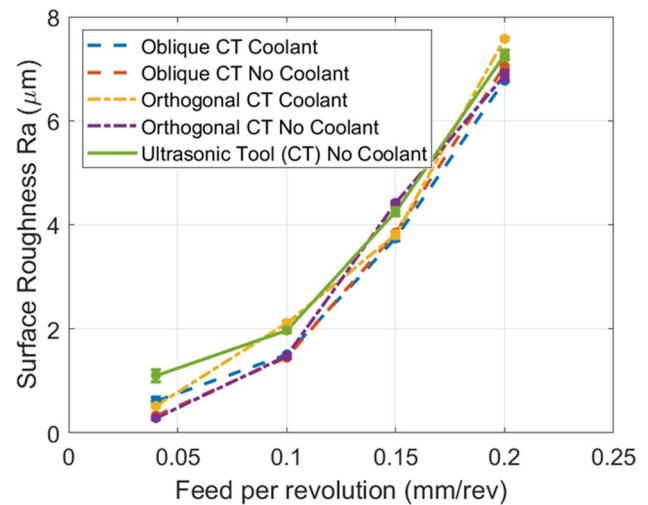


Fig. 8 Surface roughness results for benchmarking tests for cutting speed of 45 m/min at different feeds per revolution

It was clearly seen that the combined low cutting speeds produced the minimum cutting forces.

In terms of the single-assisted hybrid processes, UAM presented the highest contribution for the reduction of tangential cutting force at up to 61.6%, compared to LAM that achieved a maximum reduction of 10%. The force reduction from UAM had a greater effect in the lower range of cutting parameters. This may be related to the critical cutting speed of the ultrasonic system, which is a function of the vibration frequency and amplitude; as described by Eq. 3, where V_c is the cutting speed, f is the frequency of the ultrasonic system, and a the amplitude. This relationship shows how

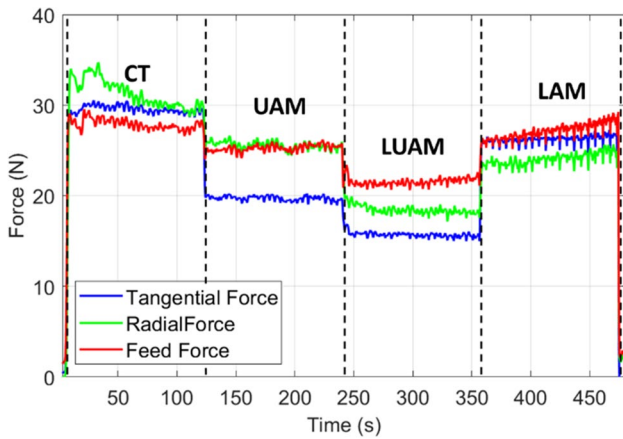


Fig. 9 Cutting force diagram of a single run (test 7) for cutting speed of 45 m/min, depth of cut of 0.2 mm, feed per revolution of 0.04 mm/rev, laser power of 750 W, and ultrasonic vibration at 20 kHz

the effect of UAM can be less effective with speeds closer to the critical value.

$$V_c = 2\pi af \tag{3}$$

The LAM process appeared to have a very marginal effect on force reduction at the different cutting speeds and depths of cut, compared to UAM. The higher performance of UAM over LAM might have been due to the machining parameters used, which were selected to benefit the ultrasonic system requirements. Another reason might be due to the thermal expansion of the material, arising from the low thermal conductivity of the Ti-6Al-4V alloy and the accumulation of heat on the workpiece, causing a slight increase in the depth of the cut. Note that the thermal expansion of the material may have also caused an increase in the radial and feed forces at the end of each cut as observed in Fig. 9.

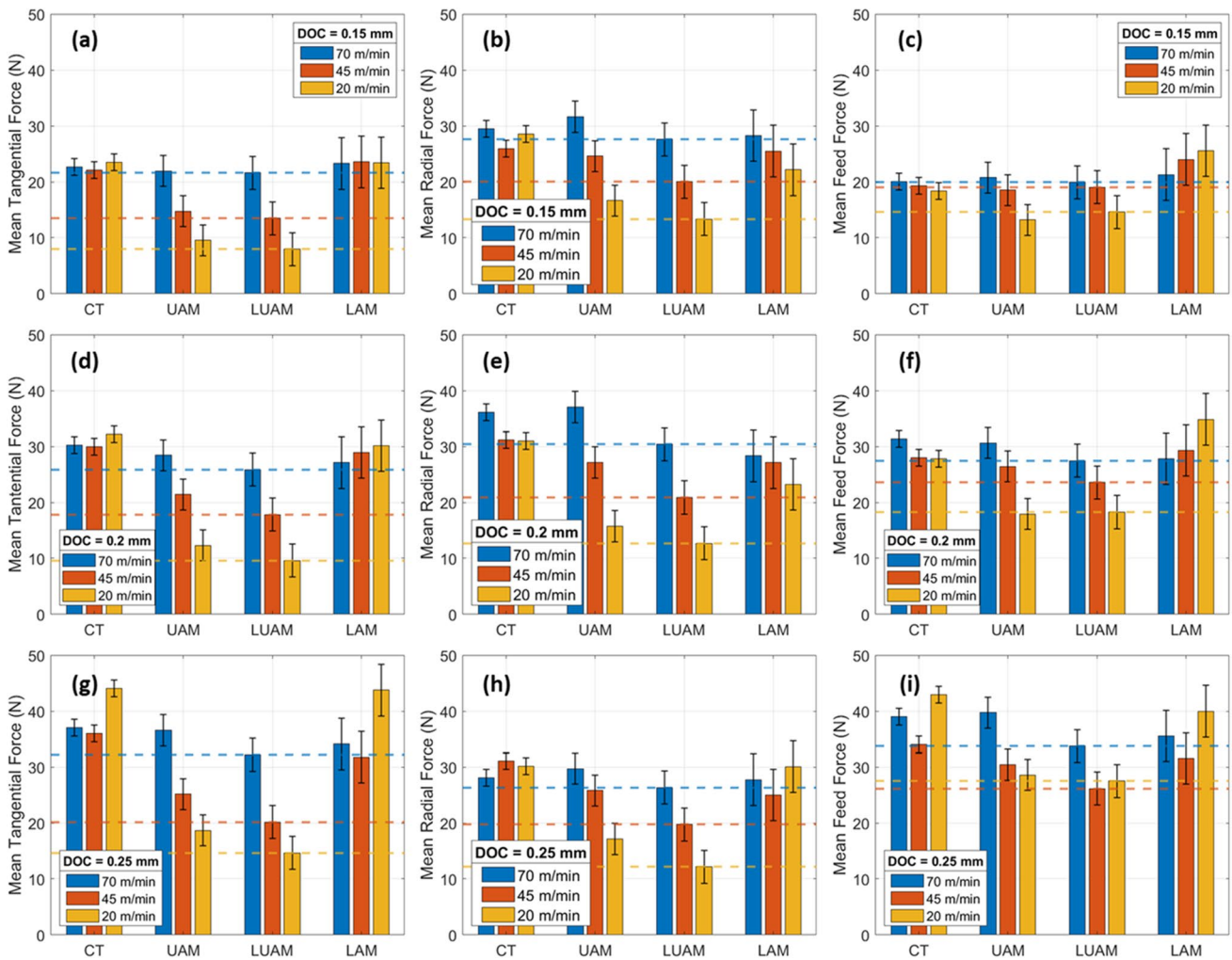


Fig. 10 Mean cutting force results for **a** DOC of 0.15 mm tangential force, **b** DOC of 0.15 mm radial force, **c** DOC of 0.15 mm feed force, **d** DOC of 0.2 mm tangential force, **e** DOC of 0.2 mm radial force, **f**

DOC of 0.2 mm feed force, **g** DOC of 0.25 mm tangential force, **h** DOC of 0.25 mm radial force, and **i** DOC of 0.25 mm feed force

The cutting test also demonstrated that the LUAM process achieved lower cutting forces for the tangential, radial, and feed force components. The combined hybrid process (LUAM) had a cumulative effect in lowering the cutting forces at a cutting speed of 20 m/min, depth of cut of 0.2 mm, and feed per revolution of 0.04 mm/rev achieving a maximum reduction of 70.1%, 59% and 43% with a confidence interval of $\pm 3\%$ in the tangential, radial, and feed forces, respectively.

The UAM system was designed for an optimal resonance frequency in the axial direction with the highest possible amplitude. As per Eq. 3, from a practical standpoint, the aim was to obtain the highest possible value of V_c to allow for rapid machining. Therefore, the effect of reducing the vibration amplitude (by adjusting the voltage) on machining forces has not been included. Prior studies [32] show that increasing the frequency and amplitude of vibrations is generally beneficial but there is a limit beyond which this benefit wanes. Thus, it is expected that improvements in the LUAM process could be achieved with an improved transducer design where the limits of resonant frequency and amplitudes are pushed further.

3.4 Hybrid turning: temperature data

The temperature data, which was acquired during the machining trials using a thermal camera, was post-processed to extract separately the temperatures from the cutting area and the laser beam incidence area. The obtained temperature data was limited to the visible portion of the cutting area, which was slightly and intermittently obstructed by the chip. Therefore, average temperature values were extracted from the thermal data.

The temperatures at the beam incidence area, as illustrated in Fig. 5, were higher for the lower speeds; however, the mean temperatures at the cutting area during LAM and LUAM processes as shown in Fig. 11a, b, and c appeared to be similar for the various cutting speeds for each depth of cut. This was probably caused by the heat dissipation before reaching the cutting tool. The top dashed black line on the graphs shows the mean temperature for the laser-assisted cuts (LAM and LUAM), and the lower dashed line corresponds to the cuts not involving the laser (CT and UAM). However, the temperature increased almost 50% from an average value of 277 °C for CT and UAM to around 550 °C for LAM and LUAM. This may explain the further reduction on cutting forces observed from LUAM as presented in the previous section. The combined effect of the mechanical and thermal softening effect from the ultrasonic and laser produced a further reduction of cutting forces.

3.5 Hybrid turning: surface roughness

Surface roughness (Ra) analysis was carried out to assess the topography of the machined surface under the selected

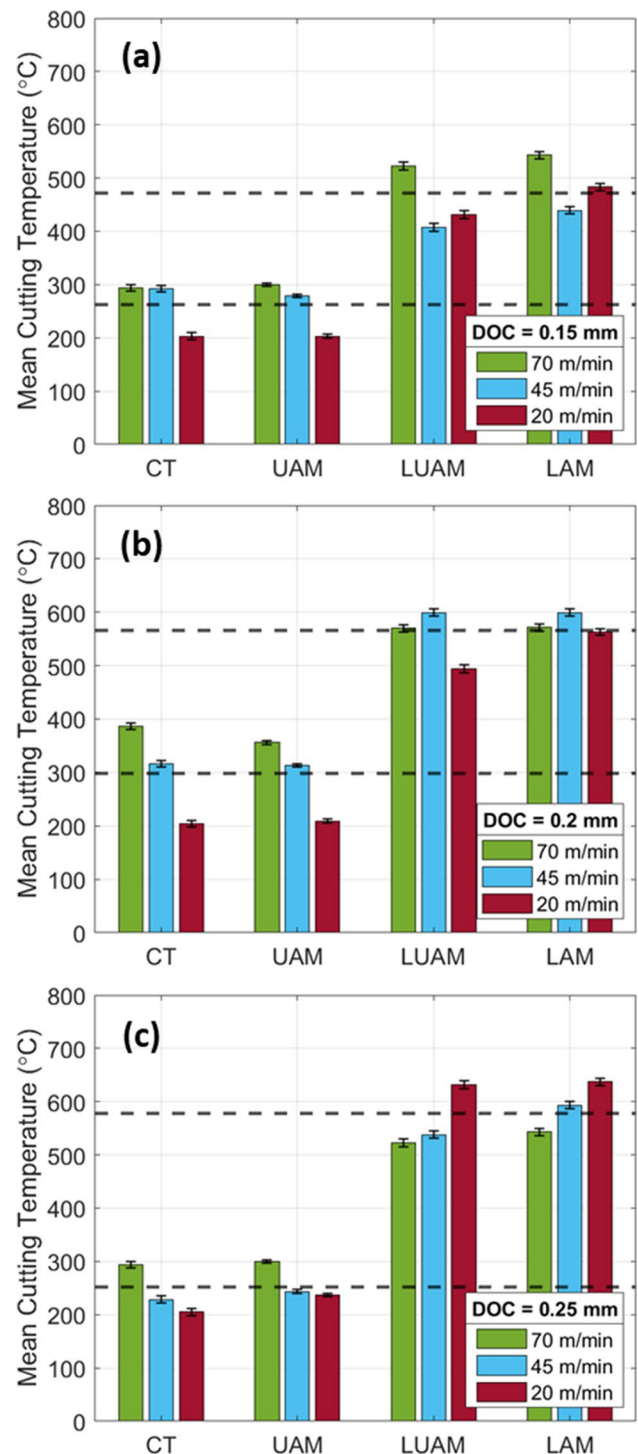


Fig. 11 Mean temperature data at the cutting-edge area across machining parameters and laser-assisted technologies for **a** DOC of 0.15 mm, **b** DOC of 0.2 mm, and **c** DOC of 0.25 mm

cutting conditions and different hybrid processes. The results from the surface roughness Ra measurements can be seen in Fig. 12. Similar to the force analysis, no data outliers were removed from the surface roughness results, which was

significant with a p value below 0 at a 95% confidence level. In general, the R_a average values for the conventional cutting tests appeared to have magnitudes nearer to $1 \mu\text{m}$. As it can be seen, there was no significant effect on the R_a values with the variation of the selected range of cutting parameters.

In the case of the single hybrid machining tests, it was clear that UAM improved the machined surface roughness (R_a) with an approximate value of $0.6 \mu\text{m}$ at the lowest speed. This was due to the greater effect of the UAM technology at the lowest range of cutting parameters as discussed in the cutting force section. It is important to note that there is a clear correlation between the reduction of the mechanical loading and the effect on the R_a ; this has been observed by other researchers [18–22] for Ti-6Al-4V. Furthermore, the reduction in mechanical loading might have also improved the stability of the cutting operation, and thus enhance the stiffness of the tool. The LAM process also exhibited a similar trend in terms of the reduction of R_a values around the same magnitudes at the lowest surface speed. As previously stated, the temperature was increased by around 50% as shown in Fig. 11, which generated a thermal softening effect on the material generating lower cutting force conditions and therefore better surface roughness.

The results revealed that the R_a was improved by the application of a LUAM process in the majority of the cutting conditions as highlighted by the dashed lines, with an exception at the speed of 70 m/min at the depths of cut of 0.15 and 0.2 mm. The LUAM appeared to produce a better surface condition (R_a) for the selected range of surface speeds and different DoC's, which was achieved due to the combined force reduction from the ultrasonic and laser assisted, as well as due to a thermal softening effect. It should be highlighted that the R_a results of the LUAM process were comparable to the robust commercial tool holder setups that were presented in the initial benchmarking in Section 3.2, regardless of the potential stiffness issue of the lab-based tool holder setup, as is illustrated in Fig. 13 for the DoC 0.25 mm. It should also be pointed out that this could have been improved further by having a more robust design of the ultrasonic tool holder. However, it was clear that LUAM further reduced the surface roughness for all conditions when compared to the CT using the ultrasonic tool holder without coolant conditions.

4 Conclusion

A Ti-6Al-4V turning process using ultrasonic- and laser-assisted machining has been investigated. The effects of a single and combined hybrid processes are experimentally evaluated by examining the cutting forces, temperatures, and surface roughness. Benchmarking was also carried out by comparing R_a values from an industrial setup of machining trials and the developed ultrasonic tool holder. The main conclusions of the study can be drawn as follows:

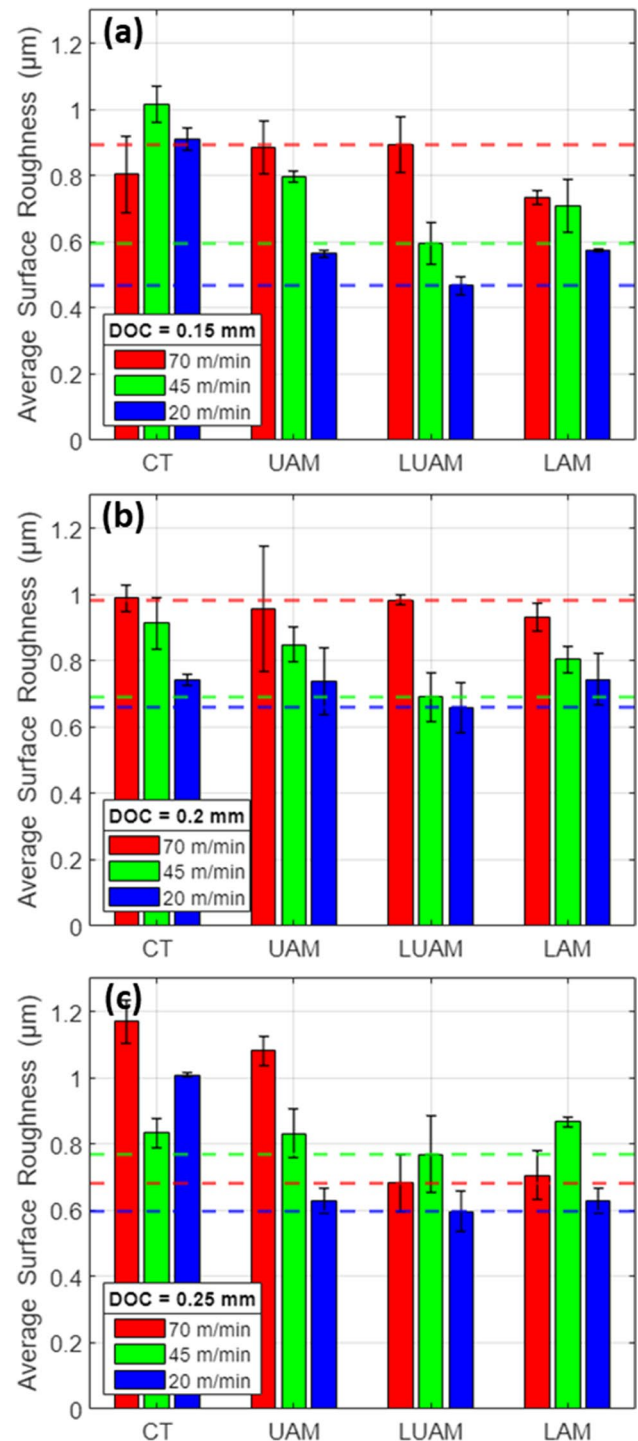


Fig. 12 Surface roughness R_a results for all assistive technologies and machining parameters for **a** DOC of 0.15 mm, **b** DOC of 0.2 mm, and **c** DOC of 0.25 mm

- 1) The temperature measurement at the laser beam incidence area, using the selected laser power of 750 W and the lowest cutting speed (20 mm/min), was higher at around $830 \text{ }^\circ\text{C}$ compared to the highest speed (70 m/

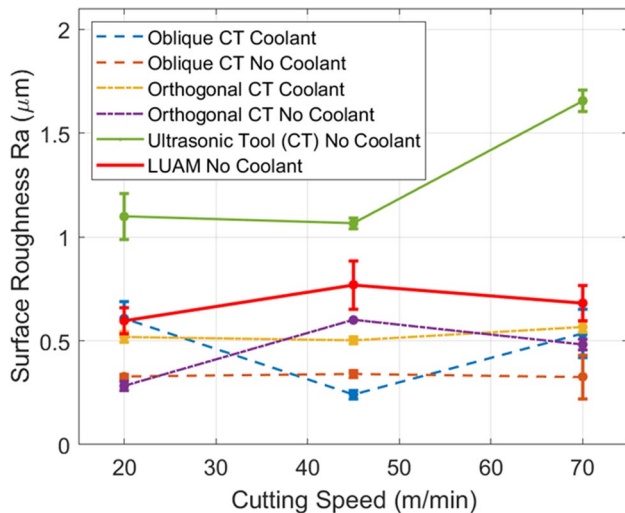


Fig. 13 Surface roughness results for benchmarking tests and LUAM technology for feed per revolution of 0.04 mm/rev at different cutting speeds

min) at about 749 °C. This was likely due to the laser beam spending a longer time in the same spot compared to that at the higher cutting speed. However, the temperature appeared to be similar for LAM and LUAM around 550 °C at the various speeds at the cutting area, which was probably caused by the heat dissipation generating similar temperature conditions.

- 2) The UAM technology presented the highest contribution for the reduction in the tangential cutting force (cutting direction) up to 61.6% as a single-assisted technology at the lowest range of cutting speed. In the case of LAM, it only achieved a maximum reduction of 10% for the same cutting direction and condition; the marginal effect on force reduction is caused by the accumulation of heat due to the low conductivity on the Ti-6Al-4V material causing an overall thermal expansion of the material, and hence potentially increasing the depth of cut and the force outcomes.
- 3) It was demonstrated that the hybrid LUAM technology achieved the lowest cutting forces for the tangential, radial, and feed force components in most of the cases. The cumulative effect in lowering the cutting forces for LUAM was most evident at the lowest cutting speed of 20 m/min for both the tangential, radial, and feed force directions, reducing them by 70.1%, 59%, and 43%, respectively with a confidence interval of $\pm 3\%$.
- 4) In terms of the surface roughness Ra, UAM and LAM processes improved the Ra to similar values between 0.7 and 0.8 μm . However, this was mainly observed at the lowest surface speed of 20 m/min.
- 5) The hybrid LUAM process demonstrates further improvement of the surface roughness (Ra around

0.7–0.8 μm) for most of the range of surface speeds (20–70 m/min) and different DoC's (0.15–0.25 mm). This was achieved due to the combined force reduction and thermal softening effect. It is worth mentioning that Ra could have been improved further by having a more robust design of the ultrasonic tool holder.

- 6) There is potential for further improvements in the laser-ultrasonically-assisted machining process with innovative transducer designs, as there were limitations in the current research in terms of the designed stiffness and working range of the ultrasonic tool holder for a closer comparison to the commercial tools. Designing transducers with higher resonance frequencies and adequate vibratory amplitudes will allow for quicker machining of materials with higher force reductions. Therefore, future work should investigate the development of a more robust design for the ultrasonic tool holder.
- 7) Finally, the research should be expanded to investigate other important indicators of a machining process such as surface integrity of the material (i.e., residual stresses, microhardness, and microstructural changes), and tool wears evolution. Similarly, analysis of the hybrid technologies should be investigated through modelling and simulation of the cutting process.

Acknowledgements This work was supported by the Engineering and Physical Science Research Council (EPSRC) Programme Grant (H2 Manufacturing: Hybrid-Hybrid machining of next generation aerospace materials) under Grant EP/P027652/1, EP/P027555/1 and EP/P027563/1.

Author contribution All authors contributed to the study conception and design. Material preparation, data collection, and analysis were performed by Javier Dominguez-Caballero and Sabino Ayvar-Soberanis. The first draft of the manuscript was written by Javier Dominguez-Caballero, Sabino Ayvar-Soberanis, and Jin Kim, and all authors reviewed and contributed on the manuscript. All authors read and approved the final manuscript.

Funding The research was funded by the Engineering and Physical Science Research Council (EPSRC) Programme Grant (H2 Manufacturing: Hybrid-Hybrid machining of next generation aerospace materials) under Grant EP/P027652/1, EP/P027555/1 and EP/P027563/1.

Data availability Data is available with the permission of University of Sheffield AMRC. The data that support the findings of this study are available from the corresponding author upon reasonable request.

Declarations

Ethical approval Not applicable

Consent to participate Not applicable

Consent for publication The authors declare that they all consent to publication.

Conflict of interest The authors declare no competing interests.

Open Access This article is licensed under a Creative Commons Attribution 4.0 International License, which permits use, sharing, adaptation, distribution and reproduction in any medium or format, as long as you give appropriate credit to the original author(s) and the source, provide a link to the Creative Commons licence, and indicate if changes were made. The images or other third party material in this article are included in the article's Creative Commons licence, unless indicated otherwise in a credit line to the material. If material is not included in the article's Creative Commons licence and your intended use is not permitted by statutory regulation or exceeds the permitted use, you will need to obtain permission directly from the copyright holder. To view a copy of this licence, visit <http://creativecommons.org/licenses/by/4.0/>.

References

- Parida AK, Maity K (2021) Study of machinability in heat-assisted machining of nickel-base alloy. *Measurement (Lond)* 170:108682. <https://doi.org/10.1016/j.measurement.2020.108682>
- He Y, Zhou Z, Zou P, Gao X, Ehmann KF (2019) Study of ultrasonic vibration-assisted thread turning of Inconel 718 superalloy. *Adv Mech Eng* 11(10):1–12. <https://doi.org/10.1177/1687814019883772>
- Bai W, Bisht A, Roy A, Suwas S, Sun R, Silberschmidt VV (2019) Improvements of machinability of aerospace-grade Inconel alloys with ultrasonically assisted hybrid machining. *Int J Adv Manuf Technol* 101(5–8):1143–1156. <https://doi.org/10.1007/s00170-018-3012-8>
- Li J, Laghari RA (2019) A review on machining and optimization of particle-reinforced metal matrix composites. *Int J Adv Manuf Technol* 100(9–12):2929–2943. <https://doi.org/10.1007/s00170-018-2837-5>
- Kim J, Bai W, Roy A, Jones LCR, Ayvar-Soberanis S, Silberschmidt VV (2019) Hybrid machining of metal-matrix composite. *Procedia CIRP* 82:184–189. <https://doi.org/10.1016/j.procir.2019.04.162>
- Bai W, Roy A, Sun R, Silberschmidt VV (2019) Enhanced machinability of SiC-reinforced metal-matrix composite with hybrid turning. *J Mater Process Technol* 268:149–161. <https://doi.org/10.1016/j.jmatprotec.2019.01.017>
- Sun J, Guo YB (2009) A comprehensive experimental study on surface integrity by end milling Ti-6Al-4V. *J Mater Process Technol* 209(8):4036–4042. <https://doi.org/10.1016/j.jmatprotec.2008.09.022>
- Sharma V, Pandey PM (2016) Recent advances in ultrasonic assisted turning: a step towards sustainability. *Cogent Eng* 3(1):1222776. <https://doi.org/10.1080/23311916.2016.1222776>
- Maurotto A, Muhammad R, Roy A, Silberschmidt VV (2013) Enhanced ultrasonically assisted turning of a β -titanium alloy. *Ultrasonics* 53(7):1242–1250. <https://doi.org/10.1016/j.ultras.2013.03.006>
- Muhammad R, Hussain MS, Maurotto A, Siemers C, Roy A, Silberschmidt VV (2014) Analysis of a free machining $\alpha+\beta$ titanium alloy using conventional and ultrasonically assisted turning. *J Mater Process Technol* 214(4):906–915. <https://doi.org/10.1016/j.jmatprotec.2013.12.002>
- Boyer RR (1996) An overview on the use of titanium in the aerospace industry. *Mater Sci Eng, A* 21(1–2):103–114. [https://doi.org/10.1016/0921-5093\(96\)10233-1](https://doi.org/10.1016/0921-5093(96)10233-1)
- Llanos I, Campa Á, Iturbe A, Arrazola PJ, Zelaieta O (2018) Experimental analysis of cutting force reduction during ultrasonic assisted turning of Ti6Al4V. *Procedia CIRP* 77:86–89. <https://doi.org/10.1016/j.procir.2018.08.227>
- Zhang J, Wang D (2019) Investigations of tangential ultrasonic vibration turning of Ti6Al4V using finite element method. *Int J Mater Form* 12(2):257–267. <https://doi.org/10.1007/s12289-018-1402-y>
- Maroju NK, Pasam VK (2019) FE modeling and experimental analysis of residual stresses in vibration assisted turning of Ti6Al4V. *Int J Precis Eng Manuf* 20(3):417–425. <https://doi.org/10.1007/s12541-019-00021-3>
- Muhammad R, Ahmed N, Ullah H, Roy A, Silberschmidt VV (2018) Hybrid machining process: experimental and numerical analysis of hot ultrasonically assisted turning. *Int J Adv Manuf Technol* 97(5–8):2173–2192. <https://doi.org/10.1007/s00170-018-2087-6>
- Gürgeç S, Çakır FH, Sofuoğlu MA, Orak S, Kuşhan MC, Li H (2019) Multi-criteria decision-making analysis of different non-traditional machining operations of Ti6Al4V. *Soft comput* 23(13):5259–5272. <https://doi.org/10.1007/s00500-019-03959-8>
- Punugupati G, Kandi KK, Bose PSC, Rao CSP (2016) Laser assisted machining: a state of art review. *IOP Conf Ser: Mater Sci Eng* 149(1):012014. <https://doi.org/10.1088/1757-899X/149/1/012014>
- Dandekar CR, Shin YC, Barnes J (2010) Machinability improvement of titanium alloy (Ti-6Al-4V) via LAM and hybrid machining. *Int J Mach Tools Manuf* 50(2):174–182. <https://doi.org/10.1016/j.ijmactools.2009.10.013>
- Kim D-H, Lee C-M (2021) Experimental investigation on machinability of titanium alloy by laser-assisted end milling. *Metals* 11(10):1552. <https://doi.org/10.3390/met11101552>
- Hedberg GK, Shin YC, Xu L (2015) Laser-assisted milling of Ti-6Al-4V with the consideration of surface integrity. *Int J Adv Manuf Technol* 79(9–12):1645–1658. <https://doi.org/10.1007/s00170-015-6942-4>
- Habrat W, Krupa K, Markopoulos AP et al (2021) Thermo-mechanical aspects of cutting forces and tool wear in the laser-assisted turning of Ti-6Al-4V titanium alloy using AlTiN coated cutting tools. *Int J Adv Manuf Technol* 115:759–775. <https://doi.org/10.1007/s00170-020-06132-w>
- Kalantari O, Jafarian F, Fallah MM (2021) Comparative investigation of surface integrity in laser assisted and conventional machining of Ti-6Al-4 V alloy. *J Manuf Process* 62:90–98. <https://doi.org/10.1016/J.JMAPRO.2020.11.032>
- Feng Y et al (2019) Residual stress prediction in laser-assisted milling considering recrystallization effects. *Int J Adv Manuf Technol* 102(1):393–402. <https://doi.org/10.1007/S00170-018-3207-Z>
- Feng Y, Hung TP, Lu YT, Lin YF, Hsu FC, Lin CF, Lu YC, Lu X, Liang SY (2019) Surface roughness modeling in laser-assisted End Milling of Inconel 718. *Mach Sci Technol* 23(4):650–668. <https://doi.org/10.1080/10910344.2019.1575407>
- Lin SY, Yang BH (2019) Experimental study of cutting performance for inconel 718 milling by various assisted machining techniques. In: *Solid State Phenomena*, vol 294. Trans Tech Publications, Ltd., pp 129–134. <https://doi.org/10.4028/www.scientific.net/ssp.294.129>
- Jiao F, Niu Y, Zhang MJ, Zhang CJ (2016) Research on characteristics of tool wear in laser heating and ultrasonic vibration cutting of tungsten carbide. *Adv Mech Eng* 8(11):1–9. <https://doi.org/10.1177/1687814016679786>
- Jiao F, Zhang MJ, Niu Y (2019) Optimization of tungsten carbide processing parameters for laser heating and ultrasonic vibration composite assisted cutting. *Proc Inst Mech Eng C J Mech Eng Sci* 233(12):4140–4153. <https://doi.org/10.1177/0954406218809123>
- Khajehzadeh M, Ahmadpoor SS, Rohani Raftar O, Beyki Sarveolia MR, Razfar MR (2021) Process parameters influence on cutting force and surface roughness during hybrid laser- and ultrasonic elliptical vibration-assisted machining. *J Braz Soc Mech Sci Eng* 43(1):32. <https://doi.org/10.1007/s40430-020-02751-2>
- Kim J, Zani L, Jones L, Roy A, Zhao L, Silberschmidt VV (2022) Hybrid-hybrid machining of SiC-reinforced aluminium metal matrix composite. *Manuf Lett* 32:63–66. <https://doi.org/10.1016/J.MFLET.2022.04.002>
- Venkatesan K, Ramanujam R, Kuppan P (2014) Laser assisted machining of difficult to cut materials: research opportunities and future directions-a comprehensive review. *Procedia Eng* 97:1626–1636. <https://doi.org/10.1016/J.PROENG.2014.12.313>

31. Sun S, Brandt M, Dargusch MS (2010) Thermally enhanced machining of hard-to-machine materials—a review. *Int J Mach Tools Manuf* 50(8):663–680. <https://doi.org/10.1016/J.IJMACHTOOLS.2010.04.008>
32. Muhammad R (2013) Hot ultrasonically assisted turning of Ti-15V3Al3Cr3Sn: experimental and numerical analysis,” Accessed: Oct. 31, 2022. [Online]. Available: <https://repository.lboro.ac.uk/>

[articles/thesis/Hot_ultrasonically_assisted_turning_of_Ti-15V3Al3Cr3Sn_experimental_and_numerical_analysis/9544304/1](https://doi.org/10.1016/J.IJMACHTOOLS.2010.04.008)

Publisher's note Springer Nature remains neutral with regard to jurisdictional claims in published maps and institutional affiliations.